Earth-Science Reviews 185 (2018) 928–937

Contents lists available at ScienceDirect

Earth-Science Reviews

journal homepage: www.elsevier.com/locate/earscirev

How autochthonous dissolved organic matter responds to eutrophication and climate warming: Evidence from a cross-continental data analysis and experiments☆

Yongqiang Zhou[a,b,c], Thomas A. Davidson[d], Xiaolong Yao[a,b], Yunlin Zhang[a,b,*], Erik Jeppesen[c,d,**], Javier Garcia de Souza[e], Huawu Wu[a,b], Kun Shi[a,b], Boqiang Qin[a,b]

[a] Taihu Laboratory for Lake Ecosystem Research, State Key Laboratory of Lake Science and Environment, Nanjing Institute of Geography and Limnology, Chinese Academy of Sciences, Nanjing 210008, China
[b] University of Chinese Academy of Sciences, Beijing 100049, China
[c] Sino-Danish Centre for Education and Research, Beijing 100190, China
[d] Department of Bioscience and Arctic Research Centre, Aarhus University, Vejlsøvej 25, DK-8600 Silkeborg, Denmark
[e] Instituto de Limnología 'Dr. Raúl A. Ringuelet' (ILPLA) (UNLP-CONICET), Boulevard 120 y 62, CC 712 La Plata, Provincia de Buenos Aires, Argentina

ARTICLE INFO

Keywords:
Chromophoric dissolved organic matter
Nutrient enrichment
Climate warming
Mesocosm
Stable isotope
Parallel factor analysis (PARAFAC)
High-resolution mass spectrometry

ABSTRACT

Harmful algal blooms have become increasingly frequent due to the dual pressure of excessive nutrient loading and climate change in recent years. Algal-derived dissolved organic matter (DOM) is a potentially large component of the labile organic matter pool, and also climate warming may affect the DOM pool, although the results on the latter so far are equivocal. The question of how eutrophication and climate warming may drive the accumulation of autochthonous DOM is much debated. Here, we analysed published data on DOM world-wide and field data that we collected from 97 lakes and major rivers in China (> 4500 samples) as well as results from the longest running shallow-lake mesocosm climate experiment in the world at a research facility in Denmark. Our results indicated that dissolved organic carbon (DOC) concentrations decreased with increasing temperature and enrichment of δ^{13}C-DOM. A negative relationship was found between latitude and %protein-like fluorescence, which increased significantly with increasing elevation and enrichment of δ^{13}C-DOM. Specific ultraviolet absorbance at 254 nm (SUVA) decreased with increasing elevation and enrichment of δ^{13}C-DOM. Fluorescence intensity of autochthonous microbial humic-like substances increased notably with eutrophication but decreased weakly with warming. DOC, biodegradable DOC, chlorophyll-*a*, δ^{13}C-DOC and autochthonous substances identified using DOM fluorescence and high resolution mass spectrometry from the mesocosm experiment were notably elevated at the high nutrient levels, while the effect of temperature was insignificant. We conclude that while eutrophication promotes DOM, warming potentially suppresses the accumulation of autochthonous DOM in inland waters.

1. Introduction

Inland waters transport, transform and store a large fraction of dissolved organic matter (DOM) received from terrestrial ecosystems and are key components of the global carbon cycle (Butman and Raymond, 2011; Feng et al., 2013; Holgerson and Raymond, 2016; Huang et al., 2018; Weyhenmeyer et al., 2015). Degradative processes that act on freshly produced DOM can produce greenhouse gases and less reactive DOM is exported downstream (Davidson et al., 2015; Kellerman et al., 2015; Maberly et al., 2012; Weyhenmeyer et al., 2012). DOM in inland waters is typically derived from soil organic matter, decaying terrestrial vegetation (i.e. litter and organic-rich layers) and autochthonous sources (e.g. phytoplankton). In productive ecosystems, autochthonous DOM derived from algal sources has a

☆ This manuscript has not been published or accepted elsewhere. We have not submitted it to any other journals. The manuscript is organized according to the format and structure of your journal.

* Correspondence to: Y. Zhang, Taihu Laboratory for Lake Ecosystem Research, State Key Laboratory of Lake Science and Environment, Nanjing Institute of Geography and Limnology, Chinese Academy of Sciences, Nanjing 210008, China.
** Correspondence to: E. Jeppesen, Department of Bioscience and Arctic Research Centre, Aarhus University, Vejlsøvej 25, DK-8600 Silkeborg, Denmark
E-mail addresses: ylzhang@niglas.ac.cn (Y. Zhang), ej@bios.au.dk (E. Jeppesen).

https://doi.org/10.1016/j.earscirev.2018.08.013
Received 9 April 2018; Received in revised form 15 August 2018; Accepted 27 August 2018
Available online 01 September 2018
0012-8252/

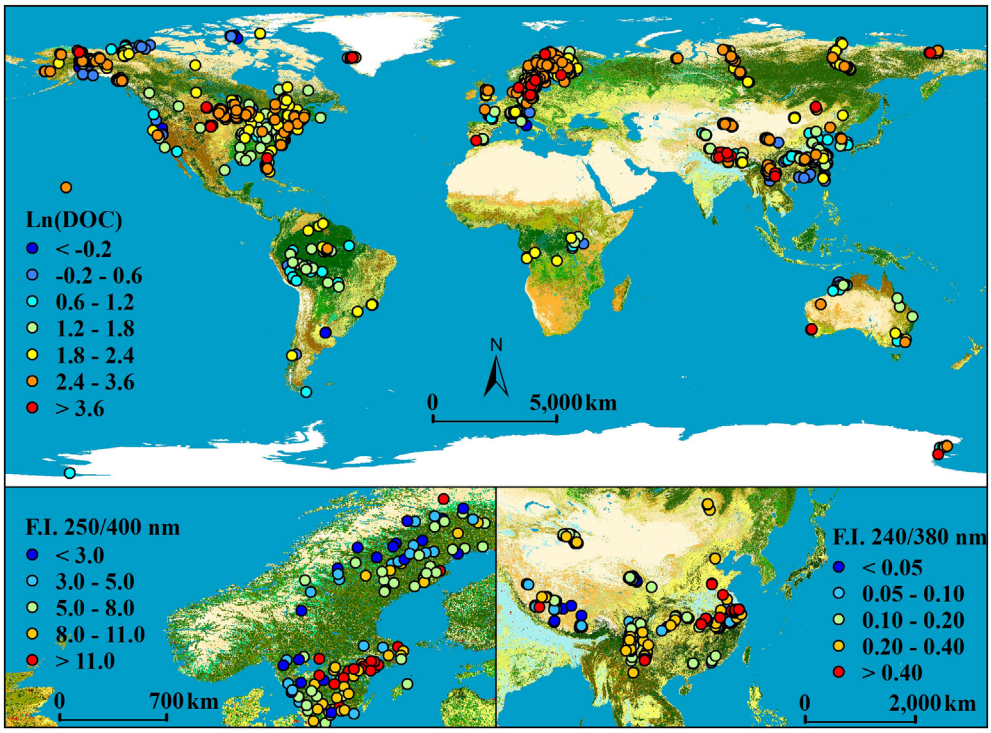

Fig. 1. Spatial distribution of natural logarithm-normalised dissolved organic carbon Ln(DOC) in inland surface waters worldwide (left panel, in mg L^{-1}, $n = 3402$). Spatial distribution of microbial-derived humic-like component (Ex/Em = 250/400 nm, in Raman Unit, upper right) in Sweden based on data obtained from Kellerman et al. (2015). Spatial variations of microbial humic-like component (Ex/Em = 240/380 nm) across China (in Raman Unit, lower right).

higher turnover than terrestrially derived DOM, the latter having already undergone some form of microbial degradation or photodegradation before entering the surface waters (Paerl and Otten, 2013). The biological DOM derived from microbial degradation of algae cells represents a considerable fraction of bio-labile DOM (Paerl and Otten, 2013). Microbial cycling of the bio-labile DOM pool has been shown to potentially fuel the outgassing of methane from lake waters (Bogard et al., 2014; Repeta et al., 2016).

The response of autochthonous DOM to the dual pressure of climate change and anthropogenic disturbance may impact the estimation of global and regional carbon budgets (Butman and Raymond, 2011). Both excess nutrients and climate change have been shown to favour dominance of cyanobacteria (Kosten et al., 2012; Paerl and Huisman, 2008) and result in accumulation of algal biomass in inland waters (Paerl and Otten, 2013; Rosemond et al., 2015), which in turn may increase the accumulation of autochthonous biological DOM. Nutrient enrichment and climate warming may further stimulate microbial reworking of particulate organic matter (POM) or terrestrial DOM precursors, augmenting the release of autochthonous DOM (Rosemond et al., 2015). Elevated temperature results in enhanced decomposition of both POM and DOM and changed sources and photo-chemical degradation during DOM transport in the aquatic continuum preferentially removing chromophoric DOM (CDOM) over the bulk dissolved organic carbon (DOC) (Hur et al., 2011a; Massicotte et al., 2017).

In forest ecosystems, nutrient enrichment has been shown to be more important than temperature in governing net primary production (Fernández-Martínez et al., 2014), and eutrophication has been revealed to override temperature in controlling greenhouse gas emissions in shallow lake ecosystems (Davidson et al., 2015). Despite significant amounts of research, the main drivers of the accumulation of autochthonous DOM remain unclear. Land use (Kellerman et al., 2014; Kellerman et al., 2015; Kothawala et al., 2014; Le et al., 2015), hydrology (Guo et al., 2014; Kellerman et al., 2014; Stedmon and Markager, 2005), temperature (Kothawala et al., 2014) and nutrients (Kellerman et al., 2014; Yao et al., 2011) have been suggested to influence the optical composition of DOM. To date, however, published results are based on studies conducted in restricted geographical areas (e.g. Sweden, China, etc.), and to the best of our knowledge, no global overview exists on the interaction effects of eutrophication and warming on DOM composition.

Climate change, eutrophication and intensified anthropogenic alterations of both terrestrial and inland aquatic ecosystems have increasingly enhanced inputs of nutrients and DOM to the receiving aquatic ecosystems (Massicotte et al., 2017). Organic and inorganic nutrients released by photochemical and biological degradation of DOM can, in turn, further enhance eutrophication of the receiving waters (Zhang et al., 2009). Microbial and photochemical degradation of DOM is constrained by its chemical composition (Kellerman et al., 2015; Spencer et al., 2014; Vonk et al., 2015), the compositional transformation of the inland water DOM pool can potentially change ecosystem functioning (Zhang et al., 2010). Integrative studies unifying existing ecosystem or site-specific knowledge of the fate and compositional dynamics of DOM across trophic and temperature gradients is therefore needed.

The objective of this study was to elucidate the relative contribution of eutrophication and climate change to boosting the accumulation of autochthonous CDOM in inland waters. Eutrophication has been repeatedly shown to transform ecosystem structure and function, whereas climate change effects are generally more subtle as increased temperature may result in both elevated primary production and respiration (Evans et al., 2006; Monteith et al., 2007; Paerl and Otten, 2013). We, therefore, hypothesised that eutrophication effects are more important in the control of the accumulation of autochthonous DOM than climate warming. Our study included three elements to assess the drivers of autochthonous CDOM in inland waters: (i) direct measurements of DOC concentrations and optical measurements (absorption and fluorescence) of CDOM in inland waters (lakes, rivers and streams) obtained from worldwide datasets comprising different climates and elevations ($n = 2637$; Fig. 1); (ii) optical measurements of a total of 1919 samples collected from 97 lakes and major rivers in China during 2005 to 2017, covering large climatic and altitudinal gradients; (iii) data collected from the longest running freshwater mesocosm climate experiment in the world conducted in Denmark.

2. Materials and methods

2.1. Data acquisition

We performed literature searches using the keywords 'dissolved organic matter', 'DOM', 'chromophoric dissolved organic matter', 'CDOM', 'dissolved organic carbon', 'DOC', 'DOM fluorescence' and either 'lake' or 'river' on Web of Science and Google Scholar in November 2017. We further searched for additional studies in the literature listed in the references of relevant papers. We also included our own dataset consisting of 1919 samples (~1000 samples with only optical measurements, i.e. CDOM absorption and fluorescence) collected from 97 lakes and major rivers in China (Fig. 1).

We included only inland water bodies (lakes and ponds with an area $> 0.01\ km^2$, rivers and streams with a width > 1 m) where the DOC concentration was reported or made available by the authors. We further excluded data collected from steady waters, including bogs and fens etc., to avoid any interference from possible point-source contaminations (wastewater or waste leachate etc.) from the watersheds. In total, direct measurements of DOM-related data from 4556 water samples (among which 3402 DOC concentrations were available) collected from inland waters worldwide were included (Fig. 1). In many studies, elevation was not reported directly but could be derived from http://haiba.qhdi.com/ based on reported longitude and latitude with a precision of < 30 m. Sampling time for most of the sites ($n = 3953$) and temperature of a limited number of sites ($n = 1355$) were obtained from the literature, and the reported temperature was validated using ArcGIS-derived multi-year (1960s–1990s) annual mean temperature obtained from http://www.worldclim.org/current (Figs. S1, S2).

2.2. Mesocosm experiment

Control experiment was undertaken using the world's longest running mesocosm experiment (since August 2003 to the present) in Lemming, Denmark (56.23°N, 9.52°E) with the aim to elucidate the effects of climate change on aquatic environments (Davidson et al., 2015; Liboriussen et al., 2005). The outdoor facility consists of 24 fully mixed, flow-through mesocosms (diameter = 1.9 m, water depth = 1 m, retention time = ~2.5 months) exposed to six different treatments: three temperature levels crossed with two nutrient concentrations, each treatment being run in four replicates. The three temperature treatments are divided into: unheated ambient temperature (AMB), the A2 scenario described by the IPCC (Houghton et al., 2001) and the A2 scenario +50% (A2+). Mean temperatures in the A2 and A2+ scenarios range from +2–4 °C to +4–6 °C, respectively, relative to AMB determined from regional downscaling of the GCM models (Davidson et al., 2015). The water temperature in the mesocosms exhibited seasonal dynamics reflecting the fluctuations in air temperature. The mesocosms include sediment collected from several lakes, which was homogenised prior to the start of the experiment in 2003, and the initial conditions for individual mesocosms were identical. All 24 mesocosms are fed by groundwater, and the low-nutrient group receives no extra nutrient addition. Mean TN and TP for the low-nutrient group are $0.23 \pm 0.06\ mg\ L^{-1}$ and $12.8 \pm 3.5\ \mu g\ L^{-1}$, respectively. In comparison, the loadings of the high-nutrient group are $7.0 \pm 0.0\ mg\ P\ m^{-2}\ day^{-1}$ and $27.1 \pm 0.0\ mg\ N\ m^{-2}\ day^{-1}$, yielding mean TN and TP concentrations in the high-nutrient group of $3.53 \pm 0.64\ mg\ L^{-1}$ and $186 \pm 40\ \mu g\ L^{-1}$, respectively (Davidson et al., 2015). The nutrient treatments typically resulted in a macrophyte-dominated clear state and an algal-dominated turbid state in the low and high nutrient mesocosms, respectively.

Water samples were collected from the mesocosms twice per day (at 07:00 and 19:00) once a week for eight weeks from June to August 2016. A total of 387 water samples (24 mesocosms × 2 times per day × 8 weeks +3 source water) were collected in acid-cleaned Niskin bottles; immediately upon collection, the samples were first filtered through pre-combusted (450 °C for 4 h) Whatman GF/F filters (0.7 μm) and then through pre-rinsed Millipore filters (0.22 μm). The chlorophyll-*a* (Chl-*a*) concentrations in the mesocosm samples collected at 07:00 in the 8-week experimental period (24 tanks × 1 time per week × 8 weeks) served as proxy for the biomass of phytoplankton.

Samples collected at 07:00 in the sixth week of the experiment were used for microbial incubation and δ^{13}C-DOC measurements to test the biolability of DOM in different treatments. We assumed that biolability of DOM and δ^{13}C-DOC in the individual mesocosms varied minimally during the mesocosm experiment as DOC and the optical measurements of DOM changed insignificantly during the experiment. Approximately 50 mL water from each sample was passed through Millipore membrane cellulose filters (0.22 μm, to remove most of the microbial biomass) and stored in 60 mL acid-cleaned bottles. The bacterial inoculums were prepared by adding to the bottles ~2 mL raw water collected from the corresponding mesocosms. The samples received nutrient amendment and were incubated at room temperature in the dark for 28 days following the method detailed in Vonk et al. (2015) and Abbott et al. (2014) and then filtered again through Millipore 0.22 μm filters. Caps were placed loosely on the bottles to avoid anoxia and the bottles were shaken gently several times every day to allow air exchange. The water volume was recorded during the incubation experiment and DOC concentrations after 28 days were adjusted for possible evaporation losses. Biodegradable DOC (BDOC, %) was calculated as the difference between the percentage before incubation and after 28 days of incubation divided by the initial DOC concentration prior to the incubation (Vonk et al., 2015).

2.3. CDOM optical spectroscopy measurements and data processing

Optical measurements of CDOM, including absorption and fluorescence, have been considered efficient and informative techniques to trace the structure and reactivity of CDOM (Coble, 2007; Kellerman et al., 2015; Murphy et al., 2008; Osburn et al., 2012; Stedmon and Markager, 2005). In our study, all samples were first filtered through pre-combusted (450 °C for 4 h) Whatman GF/F filters (0.7 μm) and then through pre-rinsed Millipore filters (0.22 μm) under low pressure for CDOM absorption and fluorescence measurements. Our field samples from lakes and major rivers in China were immediately filtered and stored in the dark at 4 °C. CDOM optical measurements were generally completed within four days after sampling as described in detail in the Supporting Information. The absorption coefficients at 254 and 350 nm, i.e. $a(254)$ and $a(350)$, which have been widely used in various studies (Kellerman et al., 2015; Spencer et al., 2012; Stedmon et al., 2015; Stedmon et al., 2007), were applied in this study as a proxy of CDOM abundance. The specific ultraviolet absorption of DOC at 254 nm (SUVA) is considered to increase with increasing aromaticity of CDOM molecules (Spencer et al., 2012). Detailed information about the measurements, calibration and normalisation (in Raman Unit, R.U.) of CDOM excitation-emission matrices (EEMs) can be found in the Supporting Information.

Humification index (HIX), defined as the ratio of fluorescence intensity integration at 435–480 nm to 300–345 nm, both excited at 254 nm (255 nm was used in this study as the spectra have excitation intervals of 5 nm), was calculated. HIX increased with increasing CDOM aromaticity (Zhou et al., 2017). Parallel factor analysis (PARAFAC) has proven a useful technique in interpreting EEMs by decomposing them into individual fluorescent components with no prior knowledge about their shape and number. For further details see the Supporting Information.

The spectral shapes of the six components were compared with published PARAFAC model results using an online spectral library called OpenFluor (Murphy et al., 2014) (Fig. 2; Fig. S3). C1 had two excitation maxima (at ≤230 and 340 nm), corresponding to a single emission maximum (460 nm) and representing terrestrial humic-like materials (Kothawala et al., 2014; Murphy et al., 2011; Stedmon et al.,

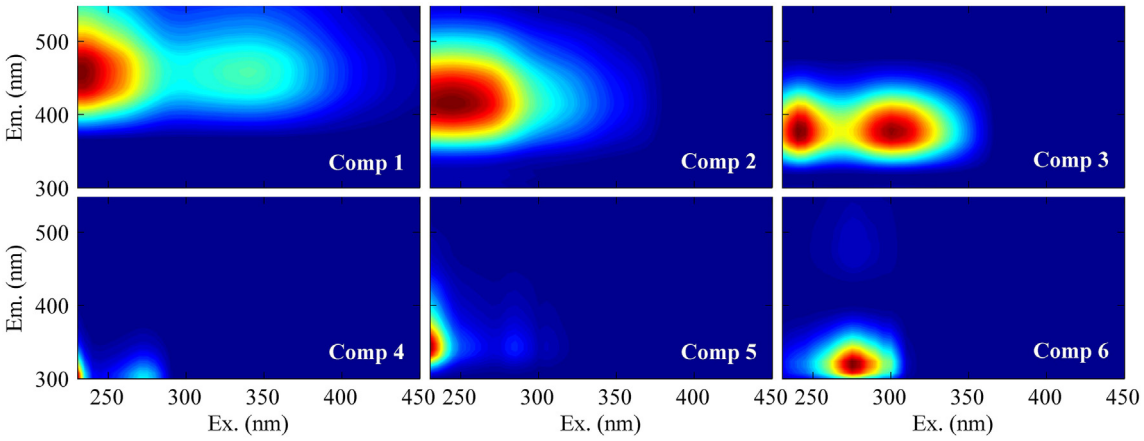

Fig. 2. Spectral characteristics of the six components identified by PARAFAC modeling. The model was validated using split-half validation procedure (Fig. S3).

2007). C2 had an excitation maximum and emission (Ex/Em = 245/412 nm) similar to those of agricultural humic-like substances or terrestrial-derived reprocessed materials (Osburn et al., 2012). C3 displayed two excitation maxima (at 240 and 300 nm) and a single emission maximum (380 nm) can be categorised as microbial humic-like compounds (Murphy et al., 2011; Osburn et al., 2011). C4 (≤ 230(270)/300 nm) showed spectral features similar to those of tyrosine-like substances (Graeber et al., 2012). C5 (≤ 230(285)/340 nm) and C6 (275/324 nm) displayed spectral shapes similar to those of tryptophan-like materials or amino acids (Murphy et al., 2013; Murphy et al., 2008). These two protein-like components (C5-C6) can be originate either from the presence of tannin-like polyphenolic moieties within the DOM (Hur et al., 2011b; Maie et al., 2007) or from algal degradation (Zhang et al., 2009).

PCA generates a reduced data array by summarising the majority of variables without prior knowledge of the dataset (Bro and Smilde, 2014). PCA for the samples collected from inland waters in China was conducted on six parameters including *a*(350), the fluorescent components C1-C3 and C5-C6. Data on the samples collected from lakes in Sweden was obtained from a reference (Kellerman et al., 2015) and reprocessed for PCA, and PCA was conducted on *a*(254), SUVA, DOC, DON, DOC:DON, HIX and the six components detailed in the reference (Kellerman et al., 2015). PCA for the mesocosm experiment was conducted on *a*(350), DOC, SUVA, HIX and the fluorescent components C1-C3 and C5-C6. All data arrays were preprocessed by autoscaling (first mean centered by subtracting the average of each column and then scaled by dividing each column by its standard deviation) prior to PCA (Bro and Smilde, 2014). PCA in this study was performed using the inbuilt statistics toolbox in MATLAB R2015b.

2.4. Fourier transform ion cyclotron resonance mass spectrometry (FT-ICR MS) and data processing

Recently, a growing number of studies have revealed that electrospray ionization coupled with high resolution mass measurements offered by Fourier transform ion cyclotron resonance mass spectrometry (FT-ICR MS) can be used to trace the dynamics of DOM at molecular level in various aquatic ecosystems (Kellerman et al., 2015; Spencer et al., 2014; Stubbins et al., 2010). Samples collected from the three temperature levels crossed with two nutrient treatments were solid-phase extracted with PPL Bond Elut (Agilent) resins before electrospray ionization FT-ICR MS (negative ion mode) (Spencer et al., 2014). Detailed information about FT-ICR MS pretreatment, measurements and calibration can be found in the Supporting Information.

The van Krevelen diagrams provide graphical plots of elemental H/C ratios against O/C ratios in molecular formulas, allowing identification of possible DOM sources (Kellerman et al., 2015; Ohno et al., 2014; Spencer et al., 2014; Stubbins et al., 2010; Zhao et al., 2017), and the biomolecular chemical classes typically include (i) lipids (O/C = 0–0.3, H/C = 1.5–2.0), (ii) proteins and amino acids (O/C = 0.3–0.67, H/C = 1.5–2.2), (iii) lignins/CRAM (O/C = 0.1–0.67, H/C = 0.7–1.5), (iv) carbohydrates (O/C = 0.67–1.2, H/C = 1.5–2.2), (v) unsaturated hydrocarbons (O/C = 0–0.1, H/C = 0.7–1.5), (vi) condensed aromatics (O/C = 0–0.67, H/C = 0.2–0.7) and (vii) tannins (O/C = 0.67–1.2, H/C = 0.5–1.5) (Ohno et al., 2014).

2.5. Stable isotopes δ^{13}C-DOC, δ^{2}H and δ^{18}O and other measurements

The stable isotope δ^{13}C-DOC can be used to investigate the sources of DOC as terrestrial humic-rich DOM usually had a δ^{13}C-DOC range from −29‰ to −26‰ and autochthonous protein-like DOM a range from −25‰ to −20‰ (Hood et al., 2009; Osburn et al., 2011; Zhou et al., 2017).

Water stable isotopes, i.e. δ^{2}H and δ^{18}O, can be used to trace the source of water as enhanced evaporation resulted in enriched δ^{2}H and δ^{18}O values (Stedmon et al., 2015; Yamamoto-Kawai, 2005). Elevated autochthonous DOM accumulation likely reduced the specific heat capacity of waters collected from the high-nutrient group and thereby resulted in an enrichment of δ^{2}H and δ^{18}O. In this study, the stable isotopes δ^{13}C-DOC, δ^{2}H and δ^{18}O of the samples collected at 5 cm depth were used in conjunction with an assessment of the compositional dynamics of CDOM in the mesocosms with different treatments (see Supporting Information for details).

Water samples were filtered through Whatman GF/F (0.7 μm) filters and DOC measurements were made using a TOC-V CPN (Shimadzu, Tokyo, Japan) analyzer by combustion at ~680 °C. The Chl-*a* concentrations were determined spectrophotometrically at 665 and 750 nm after extraction with ethanol by high speed centrifuging (3000 g for 10 min). Details about the methods used to determine total nitrogen (TN) and total phosphorous (TP) for part of the field samples collected from China can be found in Zhang et al. (2010). The trophic level index (TLI) for the samples collected from Yungui Plateau was calculated using Secchi disk depth, TN, TP and Chl-*a* (Zhang et al., 2010).

2.6. Statistical analyses

Mean, standard deviation, linear regression and *t*-test were undertaken using R-studio 0.97.551 (R i386 2.15.2) software. Spatial distribution of CDOM-related indices was determined with ArcGIS 10.2 and MATLAB R2015b software. p-value < .05 was reported as significant for linear regression and *t*-test. Mean values were obtained plus or minus their standard deviations (SD).

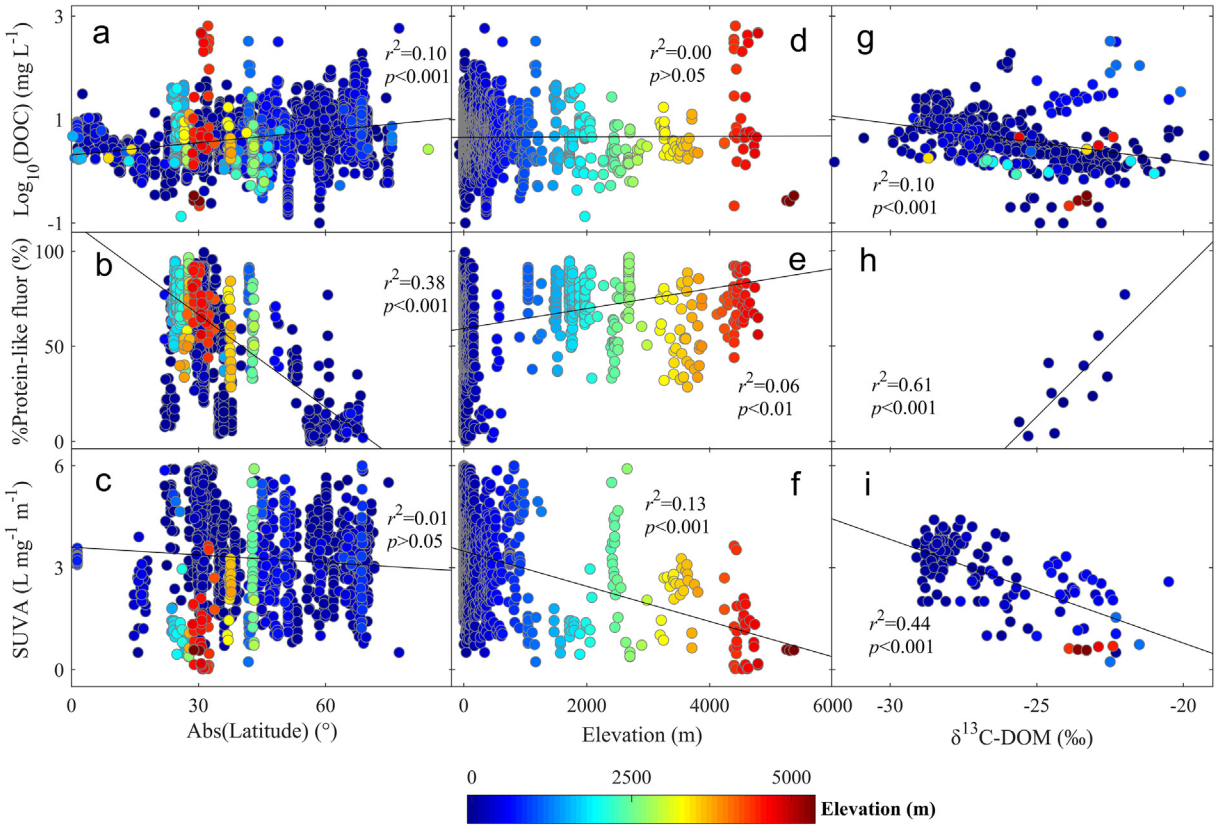

Fig. 3. Relationships between Abs(Latitude) and Log_{10}(DOC) (a), the contribution percentage of protein-like fluorescence (%protein-like fluor) (b) and the specific ultraviolet absorption at 254 nm (SUVA, c). Relationships between elevation and Log_{10}(DOC) (d), %protein-like fluor (e) and SUVA (f). Relationships between δ^{13}C-DOM and Log_{10}(DOC) (g), %protein-like fluor (h) and SUVA (i).

3. Results

3.1. General characteristics of DOM

Literature-reported and ArcGIS-derived (obtained from http://www.worldclim.org/current) temperature of all the data compiled decreased with increasing latitude and elevation (Fig. S1; Fig. S2). Approximately 45% of the compiled data were collected repeatedly from the same sites all year round (Fig. S1; Fig. S2). DOC concentrations for all sites together ranged from ~0.1 to > 100 mg L^{-1}, with the majority of the data record covering latitudes from 20°S to 70°N (Fig. 1). DOC concentrations increased significantly with increasing latitude ($p < .001$) and decreased with enrichment of δ^{13}C-DOM ($p < .001$) (Fig. 3). No significant relationship was found between elevation and DOC concentrations (Fig. 3). We found a negative relationship between the literature-reported temperature and DOC concentrations ($p < .01$), and this was validated by the relationship between multi-year (1960s–1990s) annual mean temperature (http://www.worldclim.org/current) and DOC ($p < .001$, Fig. S4). A relatively high concentration of autochthonous microbial humic-like fluorescent component (250/400 nm) was recorded in boreal and north temperate areas in Sweden (Kellerman et al., 2015) compared with temperate areas at lower latitudes (Stedmon and Markager, 2005; Zhou et al., 2017). In China, relatively high microbial humic-like C3 (240/380 nm) was recorded in eutrophic lakes in the middle and lower reaches of Yangtze River and the Yungui Plateau and in several eutrophic brine lakes in the Tibetan Plateau. Most of the sites showing high contributions of protein-like fluorescence (%protein-like fluorescence) were found between 20°N to 50°N (Fig. 3). A negative relationship was traced between latitude and %protein-like fluorescence ($p < .001$), and % protein-like fluorescence increased significantly with increasing elevation ($p < .01$) and enrichment of δ^{13}C-DOM ($p < .001$) (Fig. 3). Negative relationships also occurred between %protein-like fluorescence and the literature-reported temperature, the multi-year mean temperature derived ($p < .001$; Fig. S4). In comparison, specific ultraviolet absorbance at 254 nm (SUVA) decreased with increasing elevation and enrichment of δ^{13}C-DOM ($p < .001$) (Fig. 3). No significant relationship was discovered between latitude and SUVA (Fig. 3) or between literature-reported temperature and SUVA (Fig. S4). Our results therefore indicated, on the one hand, that increased temperature likely fuels algal blooms and thereby elevated the contribution percentage of autochthonous protein-like fluorescence and, on the other hand, enhanced the decomposition of DOC.

3.2. PCA and correlation analyses

In the PCA analysis of the PARAFAC components from field samples collected in China, the first two principal components, PC1 and PC2, explained 61.5% and 17.6%, respectively, of the variability in the data (Fig. 4a). a(350), C1-C3 and C5-C6 all showed positive PC1 loadings (Fig. 4a). This implies that PC1 is positively related to the concentration of both allochthonous and autochthonous CDOM. Relatively high scores of PC1 were recorded in eutrophic lakes in the middle and lower reaches of Yangtze River and Yungui Plateau, in eutrophic brine lakes in the Tibetan Plateau as well as in Lake Hulun and Lake Beier in northeast China (Fig. 4b). Microbial humic-like C3 increased significantly with PC1 scores ($p < .001$, Fig. 4c), and a(350) decreased with increasing elevation ($p < .001$, Fig. 4d). This indicated that eutrophication overrode temperature in enhancing the accumulation of autochthonous DOM fluorescence in Chinese lakes.

In the PCA analysis of the data obtained from (Kellerman et al., 2015) on samples collected from Sweden, PC1 and PC2 explained

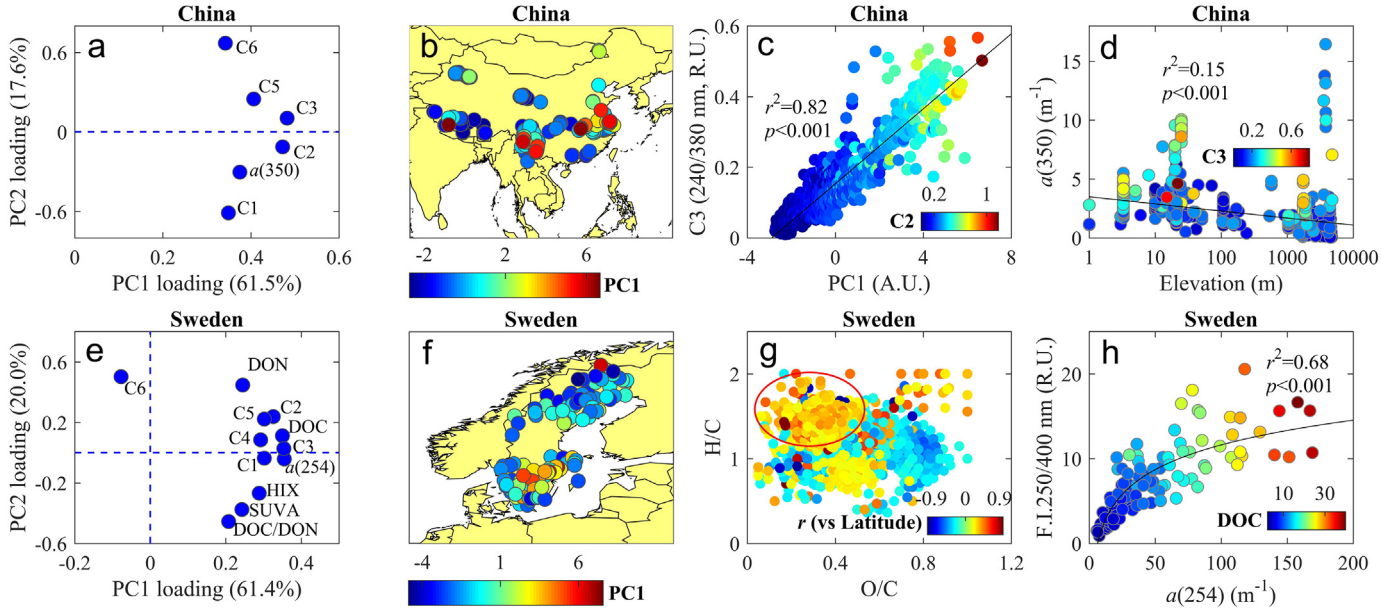

Fig. 4. PCA of the optical characteristics of CDOM samples collected from inland waters in China (a) and the corresponding spatial distribution of PC1 scores in China (b). Relationships between PC1 scores and microbial humic-like C3 for samples collected in China (c); colours denote F_{max} of agricultural humic-like C2. Relationships between Ln(Altitude) and a(350) in China (d); colours show F_{max} of C3. PCA of the optical characteristics of CDOM samples collected from lakes in Sweden (e) and the corresponding spatial distribution of PC1 scores in Sweden (f), data derived from Kellerman et al. (2015). van Krevelen diagrams for the samples collected in Sweden; colours display the r (only values of $|r| > 0.2$ were included) of Spearman correlation between the relative abundance of compounds identified by FT-ICR-MS and the latitude of the collected samples (g). Relationships between a(254) and F_{max} of an autochthonous microbial humic-like component (250/400 nm) identified by Kellerman et al. (2015); colours show DOC concentrations (mg L^{-1}).

61.4% and 20.0% of total variance. All variables except for the protein-like component C6 (Kellerman et al., 2015) displayed positive PC1 loadings (Fig. 4e). This suggests that PC1 is positively associated with the concentration of allochthonous CDOM but negatively with autochthonous CDOM. Relatively high PC1 scores were recorded in central south Sweden (Fig. 4f), while relatively low PC1 scores were found at sites located in Scandinavian mountainous areas (Fig. 4f). Significant positive relationships occurred between latitude (lower temperature) and the relative abundance of lipids and proteins or amino sugars identified by FT-ICR MS (Fig. 4g) in Sweden (Kellerman et al., 2015). This indicated that increased temperature likely enhanced the decomposition of autochthonous lipids and proteins. Close relationships were documented between the microbial component 250/400 nm and a(254) ($p < .001$, Fig. 4h) and DOC ($p < .001$, Fig. 4 h).

We recorded a significant negative relationship between elevation and ArcGIS-derived multi-year (1960s–1990s) annual mean temperature for the samples collected at the Yungui Plateau in China at elevations ranging from < 1000 m to > 4000 m ($r^2 = 0.84$, $p < .001$, Fig. S5). Autochthonous microbial humic-like C3 (240/380 nm) increased significantly with increasing TN ($r^2 = 0.74$, $p < .001$, Fig. 5a), Chl-a ($r^2 = 0.76$, $p < .001$, Fig. 5a), TP ($r^2 = 0.52$, $p < .001$) and TLI ($r^2 = 0.80$, $p < .001$, Fig. 5b), and C3 decreased significantly with increasing elevation ($r^2 = 0.13$, $p < .001$, Fig. 5c). This indicated that eutrophication rather than warming enhanced the accumulation of autochthonous C3.

3.3. Mesocosm experimental results

Notably higher mean Chl-a, DOC, a(350) and the autochthonous PARAFAC components C3, C5 and C6 were recorded in the high-nutrient in comparison with the low-nutrient group (t-test, $p < .005$, Fig. 6; Fig. S6; Table S1). No significant difference was, however, revealed between the mean of the six parameters (i.e. Chl-a, DOC, a(350), C3, C5 and C6) in different temperature scenarios with the same nutrient treatment (t-test, $p > .05$, Fig. 6; Fig. S6). The F value of two-way ANOVA analysis of the effects of nutrients is notably higher than temperature and the interaction effects of nutrient and temperature on DOC and the F_{max} of autochthonous C3 and C5 (Fig. S6; Table S2). In the PCA analysis, the first two principal components, PC1 and PC2, explained 62.9% and 22.7%, respectively, of the variability in the data array (Fig. 6). All variables, including DOC, a(350), SUVA, PARAFAC components C1-C3, C5, C6 and the HIX displayed positive loadings, which

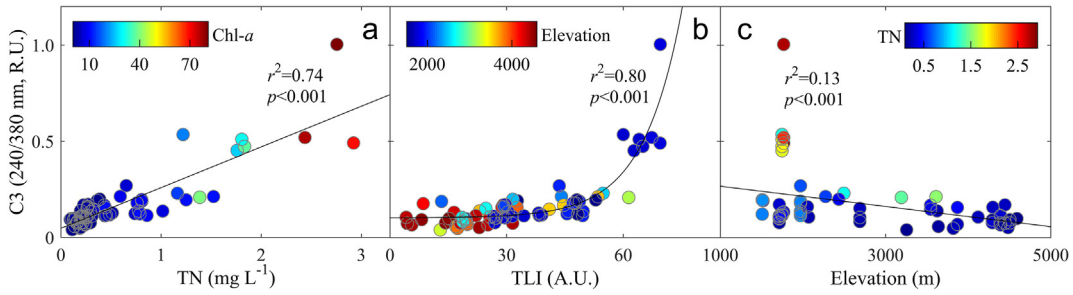

Fig. 5. Relationships between TN and microbial humic-like C3; colour denotes Chl-a concentration (μg L^{-1}, a), relationships between trophic level index (TLI) and C3; colour represents elevation (m, b), and between elevation and C3; colour stands for TN concentration (mg L^{-1}, c). The samples were collected from Yungui Plateau in China.

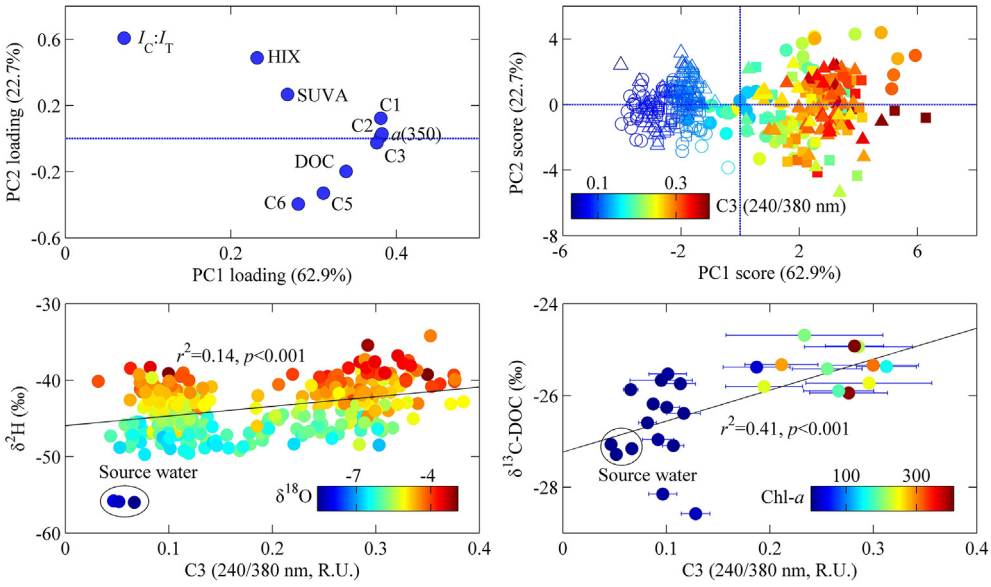

Fig. 6. Loadings (a) and scores (b) of the principal component analysis of optical characteristics of the CDOM samples collected in the mesocosm experiment. Circles: unheated ambient temperature (AMB); squares: the A2 scenario described by IPCC; triangles: A2 scenario +50% (A2+). Open and filled dots stand for low- and high-nutrient groups, respectively. Colours denote the fluorescence intensity of autochthonous microbial humic-like C3 (in R.U.). Relationships between the microbial humic-like C3 and stable isotope δ^2H; colours display δ^{18}O values (c), and between C3 and δ^{13}C-DOC, error bars are the standard deviations of C3 in each mesocosm during the 8-week sampling period. Colour denotes chlorophyll-*a* (Chl-*a*) concentrations (d).

implies that PC1 is positively related to the concentrations of autochthonous DOM as the allochthonous DOM input was identical for all mesocosms. Markedly higher PC1 scores were noted in samples from the high-nutrient group compared with the low-nutrient group (paired *t*-test, $p < .001$, Fig. 6). No significant difference was observed between the mean PC1 scores between the different temperature scenarios within the same nutrient treatment (*t*-test, $p > .05$, Fig. 6). F_{max} values of all the six components were significantly higher in the high-nutrient group than in the low-nutrient group (paired *t*-test, $p < .001$, Fig. 6, Table S1) indicating that eutrophication overrode warming in fueling the accumulation of autochthonous DOC and DOM. It is also notable that mean Chl-*a*, DOC, *a*(350) and the F_{max} values of C1, C2, C4 and C6 were lower for the A2+ treatments than for the A2 mesocosms (Table S1).

Significantly enriched mean δ^{13}C-DOC (-25.4 ± 0.4‰) was recorded for the samples from the high-nutrient group compared with those of the low-nutrient group (-26.7 ± 0.9‰) (*t*-test, $p < .005$, Table S1). Mean δ^{13}C-DOC for the source water was -27.2 ± 0.1‰ (Fig. 6). No significant difference was observed between mean δ^{13}C-DOC in the different temperature scenarios within the same nutrient treatment (*t*-test, $p > .05$, Fig. 6, Table S1). Mean δ^2H and δ^{18}O were more enriched in the samples from the high-nutrient group (-42.9 ± 3.2‰ and -5.0 ± 0.9‰, respectively) than for the low-nutrient group (-44.0 ± 6.5‰ and -5.3 ± 1.1‰, respectively) (*t*-test, $p < .005$, Table S1). Mean δ^2H and δ^{18}O of source water were -55.9 ± 0.1‰ and -8.3 ± 0.3‰, respectively. Mean δ^2H and δ^{18}O increased (became enriched) with increasing temperature (*t*-test, $p < .001$, Table S1). Significant positive relationships were recorded between the autochthonous microbial humic-like C3 and δ^2H ($r^2 = 0.14$, $p < .001$, Fig. 6) and δ^{18}O ($r^2 = 0.11$, $p < .001$, Fig. 6). Close relationships were observed between C3 and δ^{13}C-DOC ($r^2 = 0.41$, $p < .001$, Fig. 6) and between C3 and Chl-*a* ($r^2 = 0.75$, $p < .001$, Fig. 6) during the sixth week of the mesocosm experiment. There was also a close relationship between C3 and Chl-*a* ($r^2 = 0.36$, $p < .001$, Fig. S7) when all mesocosm data were pooled indicating that the microbial humic-like C3 was likely biologically produced from algal degradation.

A large fraction of autochthonous DOM accumulated in the mesocosms with extra nutrient addition was highly bio-available. BDOC ranged from 0 to 55.1% after 28 days incubation (Fig. S7) and one sample (low nutrient) was repeatedly identified as an outlier and was not considered in the further analyses. Significantly higher BDOC was recorded for the samples collected from the high-nutrient group (28.4 ± 15.7%) compared with the low-nutrient group (7.9 ± 15.8%) (*t*-test, $p < .001$, Fig. S7). Significant relationships were detected between BDOC and DOC ($r^2 = 0.57$, $p < .001$, Fig. S7) and between BDOC and F_{max} of the autochthonous microbial humic-like C3 ($r^2 = 0.41$, $p < .001$, Fig. S7). No significant impact was found of the temperature treatment on the variability of BDOC.

In this study, the DOM samples collected from different treatment mesocosms contained 5739–12,603 assigned formula peaks, and autochthonous lipids, proteins and amino acids contributed 1530–2251 peaks, or 15%–31%, of the total assigned formulas (Fig. 7; Table S3). Both the number of assigned formulas and the relative abundance of lipids, proteins and amino acids were notably higher in the high nutrient treatments than in the low nutrient treatments at all temperature levels except for the AMB group (Fig. 7; Table S3). No noticeable increase in the number of assigned formulas, contribution percentages or the relative abundance of autochthonous FT-ICR MS identified lipids, proteins and amino acids was recorded with increasing temperature (Fig. 7; Table S3). Therefore, a large fraction of biological DOM molecules accumulated in the mesocosms that receive extra nutrient addition.

4. Discussion

Our results suggest that eutrophication promotes and warming likely suppresses the accumulation of autochthonous DOM and potentially its bioavailability in inland waters.

In the mesocosm experiment, we found markedly higher mean values of δ^2H, δ^{18}O, δ^{13}C-DOC, Chl-*a*, DOC, *a*(350), autochthonous C3, C5 and C6, and higher abundance of lipids, proteins and amino-acids in the high- than the low-nutrient group for all temperature scenarios (Figs. 6–7; Fig. S6; Tables S1–S3). This supports the idea that eutrophic effects likely override those of climate warming, leading to accumulation of autochthonous DOM. Nutrient enrichment and DOM accumulation may result in a lower specific heat capacity of the water column and thereby enriched δ^2H and δ^{18}O. As the source water of the mesocosm experiment displayed depleted δ^2H, δ^{18}O and δ^{13}C-DOC signatures, the positive relationships between the microbial humic-like C3 and δ^2H, δ^{18}O and δ^{13}C-DOC (Fig. 6c-d) indicate that substantial quantities of autochthonous DOM accumulated in the high-nutrient group and markedly less in the low-nutrient group. The positive effects of eutrophication are further evidenced by the notably higher mean F_{max} of the microbial humic-like C3 in eutrophic lakes in the middle-lower Yangtze Plain and Yungui Plateau when compared with

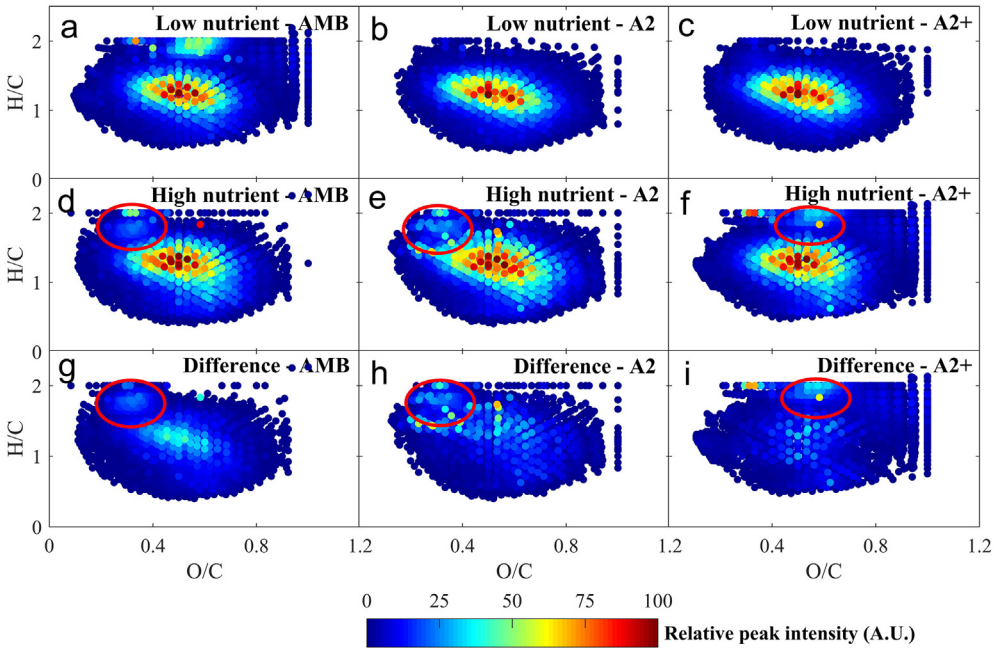

Fig. 7. van Krevelen diagrams of the distribution of DOM samples collected from the low-nutrient groups associated with unheated ambient temperature (AMB, a), the A2 scenario described by IPCC (b), the A2 scenario +50% (A2+, c) and the high-nutrient groups associated with the AMB, A2, and A2+ scenarios (d–f), the differences between the two nutrient treatment groups with different temperature scenarios (high-nutrient – low-nutrient group; g–i). In all panels, colour denotes the relative abundance of FT-ICR MS signals as a %.

oligotrophic or mesotrophic lakes in the same temperature zone (Fig. 1). In particular the significant positive relationships between microbial humic-like C3 and TN, TP, TLI and Chl-*a* for the samples collected from the Yungui Plateau, China (Fig. 5a–c), provide evidence that eutrophication is a major driver of autochthonous DOM accumulation. Furthermore, the significant association between autochthonous microbial humic-like C2 (250/400 nm) and *a*(254), a proxy of trophic level (Zhang et al., 2018), and between C2 and DOC for the Swedish samples (Fig. 4h) (Kellerman et al., 2015; Kothawala et al., 2014), point to the importance of nutrient enrichment. Increased nutrient concentrations likely lead to enhanced accumulation of DOM-rich algal biomass (Zhang et al., 2010), which develops into autochthonous labile DOM once the algal cells degrade (Paerl and Otten, 2013; Zhang et al., 2009).

Autochthonous DOM decreased with warming as increased elevation (lower temperature) resulted in enhanced autochthonous %protein-like DOM fluorescence and decreased SUVA for the globally compiled data (Fig. 3e–f). That SUVA decreased with increasing elevation (Fig. 3f) suggests a potential for enhanced degradation of humic substances and accumulation of autochthonous DOM in areas with low temperatures. This is because lower SUVA implies lower aromaticity of DOM (Zhou et al., 2017). Enhanced UV radiation at higher elevation waters can result in a higher reduction of terrestrial humic-rich substances as well as CDOM absorption relative to DOC and thereby lower SUVA and higher %protein-like DOM fluorescence (Hur et al., 2011a; Hur et al., 2011b). Previous studies have indicated that DOM in high temperature areas (tropical and subtropical areas with low elevation) was more easily decomposed and washed away (Mann et al., 2014; Spencer et al., 2016), while a large quantity of DOM was preserved in pan-Arctic and alpine areas (Drake et al., 2015) (see also Fig. 1). The lack of a direct positive temperature effect is further evidenced by the high F_{max} of the autochthonous microbial humic-like C2 (250/400 nm) in boreal areas in Sweden (Kellerman et al., 2015) and of the microbial humic-like C3 (240/380 nm) in alpine eutrophic lakes in the Yungui Plateau and the Tibetan Plateau where annual mean temperatures are generally low (Fig. 1). The close positive relationships between latitude and the relative abundance of autochthonous lipids and proteins or amino sugar molecules identified by FT-ICR MS (Fig. 4g) in Sweden further suggest that increasing temperature does not stimulate but rather reduces the accumulation of autochthonous DOM as higher temperature may enhance DOM decomposition. This is further supported by the mesocosm results where higher mean Chl-*a*, DOC, *a*(350) and F_{max} values of C1 and C2 in the A2 (+2–4 °C) than in AMB (ambient temperature) treatments in the mesocosm experiment (Table S1; Fig. S6) indicated that increased temperature enhanced phytoplanktonic primary production and thereby the DOC concentrations. However, the lower mean Chl-*a*, DOC, *a*(350) and F_{max} values of C1, C2, C4 and C6 in the A2+ (+4–6 °C than ambient) than in the A2 treatments in the mesocosm experiment (Table S1; Fig. S6) suggest that temperature effects may potentially be non-linear and there is also a possibility of enhanced decomposition and reduced accumulation of autochthonous DOM.

A large fraction of the DOM accumulated in the mesocosms with extra nutrient addition and high autochthonous DOM was highly bioavailable. This is substantiated by the notably higher BDOC in the high-nutrient than in the low-nutrient group (Table S1; Fig. S7), which is consistent with previous studies (Kellerman et al., 2015; Romera-Castillo et al., 2010; Zhang et al., 2009). The highly positive relationship between microbial humic-rich C3 and BDOC (Fig. S7) further supported the idea that at high nutrient levels, autochthonous DOM was more labile than in the low-nutrient group. Rapid microbial cycling of this fraction of bio-labile DOM probably leads to emission of greenhouse gases (Borges et al., 2015; Davidson et al., 2015; Holgerson and Raymond, 2016; Maberly et al., 2012). There are marked implications of this as the accumulation of autochthonous labile DOM serves as substrate for microbial and photochemical degradation, which may lead to greenhouse gas release (Davidson et al., 2015; Elberling et al., 2013; Maberly et al., 2012).

PARAFAC-derived microbial humic-like C3 was chosen among the six components to represent autochthonous DOM for the following reasons: (i) The spectral shape of C3 (250/380 nm) suggests that it is likely internally produced from microbial degradation of DOM-rich algae cells (Romera-Castillo et al., 2010; Zhang et al., 2009). The strong positive relationships between the microbial humic-like component (250/400 nm revealed by Kellerman et al. (2015), corresponding to C3 in this study) and the relative abundance of autochthonous lipids and proteins or amino sugars identified by FT-ICR-MS (Kellerman et al., 2015) demonstrated that this component was biologically produced. (ii) The strong positive relationships between C3 and Chl-*a*, DOC and BDOC for the field samples collected from the Yungui Plateau, China, and the

mesocosm experiment strongly suggested that C3 (Fig. 5e; Fig. S7) was produced from the degradation of algae. (iii) The significant positive relationships between C3 and the stable isotopic signatures δ^2H, $\delta^{18}O$ and $\delta^{13}C$-DOC for the mesocosm experiment provide further support of using C3 as a tracer of autochthonous DOM.

There are inevitable inter-correlations between eutrophication and warming in our global data compilation. However, the higher enrichment of autochthonous DOM in the eutrophic waters in the middle-lower Yangtze Plain and Yungui Plateau than in proximal oligotrophic or mesotrophic waters together with the greater DOM accumulation in the high-nutrient than in the low-nutrient group in the same temperature treatments provide very strong evidence that eutrophication promotes the accumulation of autochthonous DOM. Our results evidenced that the gradients of latitude and elevation can serve as reliable surrogates of temperature variabilities (Fig. S2; Fig. S5). Apparently, the effects of warming in reducing autochthonous DOM were more significant for the compiled worldwide dataset than for the mesocosm experiment (Fig. 1; Fig. 3; Fig. 6), perhaps reflecting the much larger temperature difference in the global-scale data than in the mesocosm experiment.

Autochthonous bio-labile compounds, including aliphatic substances, peptides and amino-acids associated with protein-like compounds, have been considered photoresistant, while photoreactive terrestrial humic-rich substances, aromatics and polyphenols are often thought to be biologically recalcitrant (Kellerman et al., 2014). A fraction of autochthonous DOM accumulated in inland waters due to nutrient enrichment rather than climate warming is likely to be highly bio-labile. Photochemical reactions further enhance the microbial degradation of recalcitrant DOM (Cory et al., 2014). Increased and rapid internal cycling of bio-labile and semi-labile DOM, and thereby enhanced positive feedbacks of carbon processing, can be foreseen due to excessive nutrient loading and climate warming, the dual pressures that inland waters are currently facing (Butman et al., 2014). We therefore suggest that the turnover time of DOM in watersheds with intensive land use may be significantly underestimated.

Author contributions

Y.Q.Z., T.A.D., X.Y., Y.L.Z., and E.J. conducted the research and performed the analyses. Y.Q.Z. wrote the manuscript with support from T.A.D., Y.L.Z., and E.J. All authors contributed to interpreting the results and discussions.

Competing financial interests

The authors declare no competing financial interests.

Acknowledgments

This work was supported by the National Natural Science Foundation of China (grants 41621002, 41807362, and 41771514), the Key Research Program of Frontier Sciences, Chinese Academy of Sciences (QYZDB-SSW-DQC016), the Provincial Natural Science Foundation of Jiangsu in China (BK20181104), the Strategic Priority Research Program of the Chinese Academy of Sciences (XDA19080304), and NIGLAS Foundation (NIGLAS2017GH03 and NIGLAS2017QD08). Erik Jeppesen was supported by the MARS Project (Managing Aquatic ecosystems and water Resources under multiple Stress) funded under the 7th EU Framework Programme, Theme 6 (Environment including Climate Change), Contract No.: 603378 (http://www.mars-project.eu), PROGNOS (Predicting in-lake responses to change using near real time models - Water Joint Programme Initiative) and the Centre for Water Technology (watec.au.dk). Thomas A. Davidson and Erik Jeppesen were supported by Carlsberg Foundation and the Horizon2020 project AQUACOSM (Network of Leading European AQUAtic MesoCOSM Facilities Connecting Mountains to Oceans from the Arctic to the Mediterranean) and AnaEE Denmark (anaee.dk) and AU. We would like to express our deep thanks to Anne Mette Poulsen for editorial assistance and the National High Magnetic Field Laboratory, Tallahassee, USA, for providing instrument time for the FT-ICR MS measurements. We thank Dr. Robert G.M. Spencer and Dr. David C. Podgorski for their help with FT-ICR MS measurements and their useful comments on the early version of the manuscript. The data used in this study are available upon reasonable request to the corresponding author. We thank the editor Dr. Shuhab Khan and the two anonymous reviewers for their very constructive comments.

Appendix A. Supplementary data

Supplementary data to this article can be found online at https://doi.org/10.1016/j.earscirev.2018.08.013.

References

Abbott, B.W., Larouche, J.R., Jones, J.B., Bowden, W.B., Balser, A.W., 2014. Elevated dissolved organic carbon biodegradability from thawing and collapsing permafrost. J. Geophys. Res. Biogeosci. 119 (10), 2049–2063.

Bogard, M.J., del Giorgio, P.A., Boutet, L., Chaves, M.C., Prairie, Y.T., Merante, A., Derry, A.M., 2014. Oxic water column methanogenesis as a major component of aquatic CH4 fluxes. Nat. Commun. 5, 5350.

Borges, A.V., Darchambeau, F., Teodoru, C.R., Marwick, T.R., Tamooh, F., Geeraert, N., Omengo, F.O., Guérin, F., Lambert, T., Morana, C., Okuku, E., Bouillon, S., 2015. Globally significant greenhouse-gas emissions from African inland waters. Nat. Geosci. 8 (8), 637–642.

Bro, R., Smilde, A.K., 2014. Principal component analysis. Anal. Methods 6 (9), 2812–2831.

Butman, D., Raymond, P.A., 2011. Significant efflux of carbon dioxide from streams and rivers in the United States. Nat. Geosci. 4 (12), 839–842.

Butman, D.E., Wilson, H.F., Barnes, R.T., Xenopoulos, M.A., Raymond, P.A., 2014. Increased mobilization of aged carbon to rivers by human disturbance. Nat. Geosci. 8 (2), 112–116.

Coble, P.G., 2007. Marine optical biogeochemistry: the chemistry of ocean color. Chem. Rev. 107, 402–418.

Cory, R.M., Ward, C.P., Crump, B.C., Kling, G.W., 2014. Sunlight controls water column processing of carbon in arctic fresh waters. Science 345 (6199), 925–928.

Davidson, T.A., Audet, J., Svenning, J.C., Lauridsen, T.L., Sondergaard, M., Landkildehus, F., Larsen, S.E., Jeppesen, E., 2015. Eutrophication effects on greenhouse gas fluxes from shallow-lake mesocosms override those of climate warming. Glob. Chang. Biol. 21 (12), 4449–4463.

Drake, T.W., Wickland, K.P., Spencer, R.G., McKnight, D.M., Striegl, R.G., 2015. Ancient low-molecular-weight organic acids in permafrost fuel rapid carbon dioxide production upon thaw. Proc. Natl. Acad. Sci. U. S. A. 112 (45), 13946–13951.

Elberling, B., Michelsen, A., Schädel, C., Schuur, E.A.G., Christiansen, H.H., Berg, L., Tamstorf, M.P., Sigsgaard, C., 2013. Long-term CO2 production following permafrost thaw. Nat. Clim. Chang. 3 (10), 890–894.

Evans, C.D., Chapman, P.J., Clark, J.M., Monteith, D.T., Cresser, M.S., 2006. Alternative explanations for rising dissolved organic carbon export from organic soils. Glob. Chang. Biol. 12 (11), 2044–2053.

Feng, X., Vonk, J.E., van Dongen, B.E., Gustafsson, Ö., Semiletov, I.P., Dudarev, O.V., Wang, Z., Montluçon, D.B., Wacker, L., Eglinton, T.I., 2013. Differential mobilization of terrestrial carbon pools in Eurasian Arctic river basins. Proc. Natl. Acad. Sci. U. S. A. 110 (35), 14168–14173.

Fernández-Martínez, M., Vicca, S., Janssens, I., Sardans, J., Luyssaert, S., Campioli, M., Chapin Iii, F., Ciais, P., Malhi, Y., Obersteiner, M., 2014. Nutrient availability as the key regulator of global forest carbon balance. Nat. Clim. Chang. 4 (6), 471–476.

Graeber, D., Gelbrecht, J., Pusch, M.T., Anlanger, C., von Schiller, D., 2012. Agriculture has changed the amount and composition of dissolved organic matter in Central European headwater streams. Sci. Total Environ. 438, 435–446.

Guo, W., Yang, L., Zhai, W., Chen, W., Osburn, C.L., Huang, X., Li, Y., 2014. Runoff-mediated seasonal oscillation in the dynamics of dissolved organic matter in different branches of a large bifurcated estuary-the Changjiang Estuary. J. Geophys. Res. Biogeosci. 119 (5), 776–793.

Holgerson, M.A., Raymond, P.A., 2016. Large contribution to inland water CO2 and CH4 emissions from very small ponds. Nat. Geosci. 9 (3), 222–226.

Hood, E., Fellman, J., Spencer, R.G., Hernes, P.J., Edwards, R., D'Amore, D., Scott, D., 2009. Glaciers as a source of ancient and labile organic matter to the marine environment. Nature 462 (7276), 1044–1047.

Houghton, J.T., Ding, Y., Griggs, D.J., Noguer, M., van Der Linden, P.J., Dai, X., Maskell, K., Johnson, C.A., 2001. Climate Change 2001: The Scientific Basis. Contribution of Working Group I to the Third Assessment Report of the Intergovernmental Panel on Climate Change. Cambridge University Press, Cambridge.

Huang, C., Zhang, L., Li, Y., Lin, C., Huang, T., Zhang, M., Zhu, A.x., Yang, H., Wang, X., 2018. Carbon and nitrogen burial in a plateau lake during eutrophication and phytoplankton blooms. Sci. Total Environ. 616-617, 296–304.

Hur, J., Jung, K.Y., Jung, Y.M., 2011a. Characterization of spectral responses of humic

substances upon UV irradiation using two-dimensional correlation spectroscopy. Water Res. 45 (9), 2965–2974.
Hur, J., Jung, K.Y., Schlautman, M.A., 2011b. Altering the characteristics of a leaf litter-derived humic substance by adsorptive fractionation versus simulated solar irradiation. Water Res. 45 (18), 6217–6226.
Kellerman, A.M., Dittmar, T., Kothawala, D.N., Tranvik, L.J., 2014. Chemodiversity of dissolved organic matter in lakes driven by climate and hydrology. Nat. Commun. 5, 3804.
Kellerman, A.M., Kothawala, D.N., Dittmar, T., Tranvik, L.J., 2015. Persistence of dissolved organic matter in lakes related to its molecular characteristics. Nat. Geosci. 8 (6), 454–457.
Kosten, S., Huszar, V.L.M., Bécares, E., Costa, L.S., Donk, E., Hansson, L.-A., Jeppesen, E., Kruk, C., Lacerot, G., Mazzeo, N., Meester, L., Moss, B., Lürling, M., Nõges, T., Romo, S., Scheffer, M., 2012. Warmer climates boost cyanobacterial dominance in shallow lakes. Glob. Chang. Biol. 18 (1), 118–126.
Kothawala, D.N., Stedmon, C.A., Muller, R.A., Weyhenmeyer, G.A., Kohler, S.J., Tranvik, L.J., 2014. Controls of dissolved organic matter quality: evidence from a large-scale boreal lake survey. Glob. Chang. Biol. 20 (4), 1101–1114.
Le, C., Lehrter, J.C., Hu, C., Schaeffer, B., MacIntyre, H., Hagy, J.D., Beddick, D.L., 2015. Relation between inherent optical properties and land use and land cover across Gulf Coast estuaries. Limnol. Oceanogr. 60 (3), 920–933.
Liboriussen, L., Landkildehus, F., Meerhoff, M., Bramm, M.E., Søndergaard, M., Christoffersen, K., Richardson, K., Søndergaard, M., Lauridsen, T.L., Jeppesen, E., 2005. Global warming: design of a flow-through shallow lake mesocosm climate experiment. Limnol. Oceanogr. Methods 3 (1), 1–9.
Maberly, S.C., Barker, P.A., Stott, A.W., De Ville, M.M., 2012. Catchment productivity controls CO2 emissions from lakes. Nat. Clim. Chang. 3 (4), 391–394.
Maie, N., Scully, N.M., Pisani, O., Jaffé, R., 2007. Composition of a protein-like fluorophore of dissolved organic matter in coastal wetland and estuarine ecosystems. Water Res. 41 (3), 563–570.
Mann, P.J., Spencer, R.G.M., Dinga, B.J., Poulsen, J.R., Hernes, P.J., Fiske, G., Salter, M.E., Wang, Z.A., Hoering, K.A., Six, J., Holmes, R.M., 2014. The biogeochemistry of carbon across a gradient of streams and rivers within the Congo Basin. J. Geophys. Res. Biogeosci. 119 (4), 687–702.
Massicotte, P., Asmala, E., Stedmon, C., Markager, S., 2017. Global distribution of dissolved organic matter along the aquatic continuum: across rivers, lakes and oceans. Sci. Total Environ. 609, 180–191.
Monteith, D.T., Stoddard, J.L., Evans, C.D., de Wit, H.A., Forsius, M., Hogasen, T., Wilander, A., Skjelkvale, B.L., Jeffries, D.S., Vuorenmaa, J., Keller, B., Kopacek, J., Vesely, J., 2007. Dissolved organic carbon trends resulting from changes in atmospheric deposition chemistry. Nature 450 (7169), 537–540.
Murphy, K.R., Stedmon, C.A., Waite, T.D., Ruiz, G.M., 2008. Distinguishing between terrestrial and autochthonous organic matter sources in marine environments using fluorescence spectroscopy. Mar. Chem. 108 (1–2), 40–58.
Murphy, K.R., Hambly, A., Singh, S., Henderson, R.K., Baker, A., Stuetz, R., Khan, S.J., 2011. Organic matter fluorescence in municipal water recycling schemes: toward a unified PARAFAC model. Environ. Sci. Technol. 45 (7), 2909–2916.
Murphy, K.R., Stedmon, C.A., Graeber, D., Bro, R., 2013. Fluorescence spectroscopy and multi-way techniques. PARAFAC. Anal. Methods 5 (23), 6557–6566.
Murphy, K.R., Stedmon, C.A., Wenig, P., Bro, R., 2014. OpenFluor–an online spectral library of auto-fluorescence by organic compounds in the environment. Anal. Methods 6 (3), 658–661.
Ohno, T., Parr, T.B., Gruselle, M.C., Fernandez, I.J., Sleighter, R.L., Hatcher, P.G., 2014. Molecular composition and biodegradability of soil organic matter: a case study comparing two new England forest types. Environ. Sci. Technol. 48 (13), 7229–7236.
Osburn, C.L., Wigdahl, C.R., Fritz, S.C., Saros, J.E., 2011. Dissolved organic matter composition and photoreactivity in prairie lakes of the U.S. Great Plains. Limnol. Oceanogr. 56 (6), 2371–2390.
Osburn, C.L., Handsel, L.T., Mikan, M.P., Paerl, H.W., Montgomery, M.T., 2012. Fluorescence tracking of dissolved and particulate organic matter quality in a river-dominated estuary. Environ. Sci. Technol. 46 (16), 8628–8636.
Paerl, H.W., Huisman, J., 2008. Climate. Blooms like it hot. Science 320, 57–58.
Paerl, H.W., Otten, T.G., 2013. Environmental science. Blooms bite the hand that feeds them. Science 342 (6157), 433–434.
Repeta, D.J., Ferrón, S., Sosa, O.A., Johnson, C.G., Repeta, L.D., Acker, M., Delong, E.F., Karl, D.M., 2016. Marine methane paradox explained by bacterial degradation of dissolved organic matter. Nat. Geosci. 9 (12), 884–887.
Romera-Castillo, C., Sarmento, H., Álvarez-Salgado, X.A., Gasol, J.M., Marrasé, C., 2010. Production of chromophoric dissolved organic matter by marine phytoplankton. Limnol. Oceanogr. 55 (1), 446–454.
Rosemond, A.D., Benstead, J.P., Bumpers, P.M., Gulis, V., Kominoski, J.S., Manning, D.W.P., Suberkropp, K., Bruce, W.J., 2015. Experimental nutrient additions accelerate terrestrial carbon loss from stream ecosystems. Science 347, 1142–1145.
Spencer, R.G.M., Butler, K.D., Aiken, G.R., 2012. Dissolved organic carbon and chromophoric dissolved organic matter properties of rivers in the USA. J. Geophys. Res. 117, G03001.
Spencer, R.G.M., Guo, W., Raymond, P.A., Dittmar, T., Hood, E., Fellman, J., Stubbins, A., 2014. Source and biolability of ancient dissolved organic matter in glacier and lake ecosystems on the Tibetan Plateau. Geochim. Cosmochim. Acta 142, 64–74.
Spencer, R.G.M., Hernes, P.J., Dinga, B., Wabakanghanzi, J.N., Drake, T.W., Six, J., 2016. Origins, seasonality, and fluxes of organic matter in the Congo River. Glob. Biogeochem. Cycles 30 (7), 1105–1121.
Stedmon, C.A., Markager, S., 2005. Resolving the variability in dissolved organic matter fluorescence in a temperate estuary and its catchment using PARAFAC analysis. Limnol. Oceanogr. 50 (2), 686–697.
Stedmon, C.A., Thomas, D.N., Granskog, M., Kaartokallio, H., Papadimitriou, S., Kuosa, H., 2007. Characteristics of dissolved organic matter in Baltic coastal sea ice: allochthonous or autochthonous origins? Environ. Sci. Technol. 41 (21), 7273–7279.
Stedmon, C.A., Granskog, M., Dodd, P.A., 2015. An approach to estimate the freshwater contribution from glacial melt and precipitation in East Greenland shelf waters using colored dissolved organic matter (CDOM). J. Geophys. Res. Oceans 120, 1107–1117.
Stubbins, A., Spencer, R.G.M., Chen, H., Hatcher, P.G., Mopper, K., Hernes, P.J., Mwamba, V.L., Mangangu, A.M., Wabakanghanzi, J.N., Six, J., 2010. Illuminated darkness: Molecular signatures of Congo River dissolved organic matter and its photochemical alteration as revealed by ultrahigh precision mass spectrometry. Limnol. Oceanogr. 55 (4), 1467–1477.
Vonk, J.E., Tank, S.E., Mann, P.J., Spencer, R.G.M., Treat, C.C., Striegl, R.G., Abbott, B.W., Wickland, K.P., 2015. Biodegradability of dissolved organic carbon in permafrost soils and aquatic systems: a meta-analysis. Biogeosciences 12 (23), 6915–6930.
Weyhenmeyer, G.A., Fröberg, M., Karltun, E., Khalili, M., Kothawala, D., Temnerud, J., Tranvik, L.J., 2012. Selective decay of terrestrial organic carbon during transport from land to sea. Glob. Chang. Biol. 18 (1), 349–355.
Weyhenmeyer, G.A., Kosten, S., Wallin, M.B., Tranvik, L.J., Jeppesen, E., Roland, F., 2015. Significant fraction of CO2 emissions from boreal lakes derived from hydrologic inorganic carbon inputs. Nat. Geosci. 8, 933–936.
Yamamoto-Kawai, M., 2005. Freshwater and brine behaviors in the Arctic Ocean deduced from historical data of δ18O and alkalinity (1929–2002 A.D.). J. Geophys. Res. 110, C10003.
Yao, X., Zhang, Y., Zhu, G., Qin, B., Feng, L., Cai, L., Gao, G., 2011. Resolving the variability of CDOM fluorescence to differentiate the sources and fate of DOM in Lake Taihu and its tributaries. Chemosphere 82 (2), 145–155.
Zhang, Y., van Dijk, M.A., Liu, M., Zhu, G., Qin, B., 2009. The contribution of phytoplankton degradation to chromophoric dissolved organic matter (CDOM) in eutrophic shallow lakes: field and experimental evidence. Water Res. 43 (18), 4685–4697.
Zhang, Y.L., Zhang, E.L., Yin, Y., van Dijk, M.A., Feng, L.Q., Shi, Z.Q., Liu, M.L., Qin, B.Q., 2010. Characteristics and sources of chromophoric dissolved organic matter in lakes of the Yungui Plateau, China, differing in trophic state and altitude. Limnol. Oceanogr. 55 (6), 2645–2659.
Zhang, Y., Zhou, Y., Shi, K., Qin, B., Yao, X., Zhang, Y., 2018. Optical properties and composition changes in chromophoric dissolved organic matter along trophic gradients: implications for monitoring and assessing lake eutrophication. Water Res. 131, 255–263.
Zhao, Z., Gonsior, M., Luek, J., Timko, S., Ianiri, H., Hertkorn, N., Schmitt-Kopplin, P., Fang, X., Zeng, Q., Jiao, N., Chen, F., 2017. Picocyanobacteria and deep-ocean fluorescent dissolved organic matter share similar optical properties. Nat. Commun. 8, 15284.
Zhou, Y., Shi, K., Zhang, Y., Jeppesen, E., Liu, X., Zhou, Q., Wu, H., Tang, X., Zhu, G., 2017. Fluorescence peak integration ratio IC:IT as a new potential indicator tracing the compositional changes in chromophoric dissolved organic matter. Sci. Total Environ. 574, 1588–1598.